

			Form Approved OMB NO. 0704-0188	
Public Reporting burden for this collection of information is estimated to average 1 hour per response, including the time for reviewing instructions, searching existing data sources, gathering and maintaining the data needed, and completing and reviewing the collection of information. Send comment regarding this burden estimates or any other aspect of this collection of information, including suggestions for reducing this burden, to Washington Headquarters Services, Directorate for information Operations and Reports, 1215 Jefferson Davis Highway, Suite 1204, Arlington, VA 22202-4302, and to the Office of Management and Budget, Paperwork Reduction Project (0704-0188,) Washington, DC 20503.				
1. AGENCY USE ONLY (Leave Blank)		2. REPORT DATE 20-Nov-2006		3. REPORT TYPE AND DATES COVERED Final Report, 01-Jun-2006 - 31-Jan-2007
4. TITLE AND SUBTITLE Functionally graded shape memory alloy composites optimized for passive vibration control			5. FUNDING NUMBERS W911NF-06-1-0189	
6. AUTHOR(S) Victor Birman				
7. PERFORMING ORGANIZATION NAME(S) AND ADDRESS(ES) Engineering Education Center; University of Missouri - Rolla; 101 ME Annex; 1807 Miner Circle; Rolla, MO 65409-1330			8. PERFORMING ORGANIZATION REPORT NUMBER	
9. SPONSORING / MONITORING AGENCY NAME(S) AND ADDRESS(ES) U. S. Army Research Office P.O. Box 12211 Research Triangle Park, NC 27709-2211			10. SPONSORING / MONITORING AGENCY REPORT NUMBER 49634.2-EG-II	
11. SUPPLEMENTARY NOTES The views, opinions and/or findings contained in this report are those of the author(s) and should not be construed as an official Department of the Army position, policy or decision, unless so designated by other documentation.				
12 a. DISTRIBUTION / AVAILABILITY STATEMENT Approved for public release; distribution unlimited.			12 b. DISTRIBUTION CODE	
13. ABSTRACT (Maximum 200 words) The author has developed a methodology for the dynamic analysis of composite and isotropic plates supported by functionally graded shape memory alloy wires embedded in sleeves. The solution of the equations of motion is obtained for shear deformable plates using the first order shear deformation theory and for thin plates by the classical plate theory. Two designs of functionally graded shape memory alloy reinforcements are considered, including wires in sleeves that are continuously bonded to the surface of the plate and wires attached to the plate at selected points. Numerical computations confirm that strategically placed shape memory alloy wires supporting composite and isotropic plates can serve as an effective tool for the reduction of amplitudes of forced vibrations. The wires do not reduce the amplitude of motion for an arbitrary value of the driving frequency. Instead, they effectively shift the resonance frequencies of the plate to larger values. Thus, they should be used selectively, only in applications where the spectrum of driving frequencies is known in advance.				
14. SUBJECT TERMS linear vibrations, superelastic shape memory alloy wires, forced vibrations, hysteresis			15. NUMBER OF PAGES 23 pages	
			16. PRICE CODE	
17. SECURITY CLASSIFICATION OR REPORT UNCLASSIFIED	18. SECURITY CLASSIFICATION ON THIS PAGE UNCLASSIFIED	19. SECURITY CLASSIFICATION OF ABSTRACT UNCLASSIFIED	20. LIMITATION OF ABSTRACT UL	

NSN 7540-01-280-5500

Standard Form 298 (Rev.2-89)
Prescribed by ANSI Std. Z39-18
298-102

Enclosure 1

1. Introduction

Shape memory alloy (SMA) elements have been considered for control of vibrations as well as for the enhancement of stability of composite and metallic plates by numerous investigators. The early work in this direction has been reviewed by the author¹. In general, a reduction of vibration amplitudes using SMA can be achieved through two mechanisms. SMA fibers or wires prestressed through a phase transformation can apply tensile forces to the structure increasing its effective stiffness. If SMA elements operate in the superelastic regime, their large hysteresis loop corresponding to a significant energy dissipation per cycle of motion can also be employed to reduce dynamic deformations.

The method used to reduce dynamic response or enhance stability is often based on embedding SMA fibers within the structure. Some of the studies concerned with embedding fibers bonded to the composite substrate are referred to in¹; a comprehensive review of this subject is outside the scope of this paper. Investigations of the effect of SMA wires embedded in sleeves preventing direct contact between SMA and the substrate were initiated by Baz and his collaborators. For example, multiple dynamic problems of composite structures reinforced with such wires in sleeves were considered in^{2,3}. Embedding SMA wires in sleeves provides a number of advantages, including an ease of activation and a reduction of the effect of temperature changes in the wire on the adjacent composite structure. A further improvement can be achieved by placing the sleeves outside the structure, i.e. bonding them to the surface, rather than embedding within the structure⁴. Externally bonded to the structure sleeves with SMA wires serve as an equivalent elastic foundation resisting deflections of the structure.

As indicated above, the dissipation of energy in a superelastic SMA wire results in a reduction of the dynamic response. The hysteresis loop of SMA is very large but the complete hysteresis can only be achieved if the strain reaches several percents. Although such large hysteresis loop is unlikely to be useful in plates and shells, dampers utilizing the complete superelastic hysteresis have been considered for civil engineering applications⁵ and in spring-mass isolation systems⁶. In the present problem, superelastic wires undergo an incomplete hysteresis (inner hysteresis loop). Accordingly, when it comes to the control of forced vibrations, the dissipation of energy may be a secondary effect compared to the resistance of stretched wires to deflections of the structure. Nevertheless, the following solution can account for both phenomena.

The solution presented in the paper refers to a shear deformable composite plate analyzed by a first-order theory. The particular case of a thin plate treated by the classical plate theory is also presented.

2. Analysis

Consider a shear deformable rectangular plate with SMA wires in sleeves bonded to one of the surfaces as shown in Fig. 1. SMA wires can freely slide along the sleeves, i.e. friction is negligible. One of the advantages of such design compared to embedding SMA

fibers in sleeves within the structure is related to the ease of manufacture. In addition, external sleeves do not compromise the integrity of the composite structure as may be the case if they were embedded. The issues of maintenance and joining SMA wires to supports are also easier solved in the configuration considered here. Bonding the sleeves at selected locations to the structure results in a selective transfer of the reactions as described below in the paper optimizing the effect of SMA wires on the response. It is assumed that the stiffness of the sleeve material is small, i.e. the sleeves do not affect the matrix of stiffnesses of the plate. If necessary, this requirement can be enforced by cutting the sleeves at periodic, closely spaced intervals. In the unlikely case where it is necessary to account for the contribution of the sleeves, the method enabling us to incorporate their stiffness in the analysis can be based on standard discrete stiffener method or in case of closely spaced sleeves, on the smeared stiffeners technique⁷. The contribution of the sleeves and SMA wires to the inertial coefficients is included in the present solution.

Prior to the installation, a SMA wire is cooled so that the material is transformed into martensite and stretched to a required length. Subsequently, it is inserted in the sleeves and constrained by joining it to the supporting structure. As temperature returns to the operational level corresponding to the austenitic phase of SMA, the wire is in tension as a result of constrained recovery, while the supporting structure resists the reactive forces. Such approach has been introduced and applied in numerous references reviewed in Introduction. As is shown in Fig. 1, two mutually perpendicular systems of wires oriented along the edges of the plate overlap. Several methods of design of such overlapping systems could be suggested but these details are outside the scope of this paper (of course, desirable results could also be achieved using a single system of wires oriented along either x or y directions).

As was shown by Epps and Chandra on the example of a beam, the effect of a stretched wire that can freely slide within the sleeve continuously bonded to the vibrating structure is equivalent to an elastic foundation with the stiffness varying along the wire⁴. In the present paper, we formulate the problem of an optimal distribution of SMA wires bonded to the plate either continuously or at selected points with the goal of reducing the dynamic response to a prescribed level. The design approach considered in the paper provides the following advantages:

1. Optimizing the distribution of SMA wires (or attaching the sleeves to the plate at appropriately selected points) it is possible to minimize the number of wires and maximize their effectiveness, while reducing the reactive force that is applied to the supporting structure. As a result the weight of the plate and wires can be reduced.
2. The wires located in the sleeves outside the body of the plate can be activated thermally on the “as needed” basis, without significant heat transfer to the plate. Accordingly, the reactive force applied to the supporting structure will be generated only during time intervals when the plate experiences significant vibrations (the SMA wire can remain in the martensite phase at other time intervals).

It is noted that the amplitude of forced vibrations of the plate is reduced due to two mechanisms:

1. The “elastic foundation” or “elastic supports” provided by stretched SMA wires;
2. Superelastic hysteresis in a SMA wire when it experiences vibrations. The strain range of a typical vibrating structure being relatively small compared to the range needed for a complete hysteresis loop in such SMA as Nitinol, it is anticipated that the wire can only experience an incomplete hysteresis.

2.1. SMA wires in sleeves continuously bonded to the plate

It is assumed that the plate considered in the analysis is symmetric about its middle plane. Accordingly, the equations of motion can be obtained as an extension of the equations for a shear deformable plate without an elastic foundation presented in numerous references, such as the monograph of Reddy⁸:

$$\begin{aligned}
 A_{55}(w_{,xx} + \phi_{x,x}) + A_{44}(w_{,yy} + \phi_{y,y}) - [k_1(x, y) + k_2(x, y)]w + q(x, y, t) &= m(x, y)\ddot{w} + [c_1(y) + c_2(x)]\dot{w} \\
 D_{11}\phi_{x,xx} + D_{66}\phi_{x,yy} + (D_{12} + D_{66})\phi_{y,xy} - A_{55}(w_{,x} + \phi_x) &= I(x, y)\ddot{\phi}_x \\
 D_{22}\phi_{y,yy} + D_{66}\phi_{y,xx} + (D_{12} + D_{66})\phi_{x,xy} - A_{44}(w_{,y} + \phi_y) &= I(x, y)\ddot{\phi}_y
 \end{aligned} \tag{1}$$

where the extensional (A_{ij}) and bending (D_{ij}) stiffness coefficients are defined in the customary manner and q is the applied dynamic pressure. The stiffness terms A_{44}, A_{55} incorporate the shear correction factor. The stiffness of the equivalent elastic foundations produced by the systems of wires oriented in the y and x directions are denoted by $k_1(x, y)$ and $k_2(x, y)$, respectively, while $c_1(y), c_2(x)$ are equivalent viscous damping coefficients of the corresponding systems of wires. The derivation of $k_1(x, y), k_2(x, y)$ and $c_1(y), c_2(x)$ is shown below.

The inertial terms include the mass per unit surface area of the plate that can be calculated accounting for the weight of sleeves and wires and using the analogy to the smeared stiffeners technique:

$$m(x, y) = \rho_p h + \frac{\rho_w A_y + \rho_s A_{sy}}{l_x} + \frac{\rho_w A_x + \rho_s A_{sx}}{l_y} \tag{2}$$

where ρ_p, ρ_w and ρ_s denote the mass density of the plate, wire and sleeve materials, respectively, h is the thickness of the plate, and $l_x = l_x(x)$ and $l_y = l_y(y)$ are spacings of the systems of wires oriented in the y and x directions, respectively (see Fig. 1). The cross sectional areas of the wires oriented in the y and x directions and the cross sectional areas of the sleeves encompassing these wires are denoted by A_y, A_x, A_{sy} and A_{sx} .

The rotational inertia can also be evaluated “smearing” the wires in sleeves over the surface of the plate, so that

$$I(x, y) = \int \rho_p z^2 dz + \frac{\rho_w I_y + \rho_s I_{sy}}{l_x} + \frac{\rho_w I_x + \rho_s I_{sx}}{l_y} \quad (3)$$

In (3), the integration is conducted through the thickness of the plate, while I_y , I_{sy} , I_x , I_{sx} denote the moments of inertia of respective wires and sleeves about the middle plane of the plate.

The damping coefficient of a system of wires can be determined in terms of the coefficient of a single wire C_w . Then the smeared damping of the systems of wires in the x and y direction is

$$c_1 = \frac{C_{wx}}{l_y} \quad c_2 = \frac{C_{wy}}{l_x} \quad (4)$$

where C_{wx} and C_{wy} represent damping produced in a single wire oriented in the x and y directions, respectively.

In the areas of the plate where the distance between the wires is large smearing the inertial and damping effects may become inaccurate so that each wire has to be accounted for individually. This can be accomplished by replacing the spacing in (2), (3) and (4) with a Dirac delta function, so that $\frac{1}{l_x} \rightarrow \delta(x - x_i)$, $\frac{1}{l_y} \rightarrow \delta(y - y_j)$, x_i and y_j being the coordinates of the corresponding wire.

The stiffness of the foundation modeling the effect of a system of wires is now derived expanding the solution for a single wire by Epps and Chandra⁴. The bending stiffness of the wire could be accounted for but it is negligible in realistic design applications. The bending moment acting at a cross section $x = \xi$ of a wire oriented in the x-direction, stretched by a tensile force T and subject to a concentrated force Q as shown in Fig. 2 is

$$M = \frac{Q(a - \xi)}{a} x - Tw - [Q(x - \xi)]_{x \geq \xi} \quad (5)$$

The negligible bending stiffness of the wire implies that this moment is equal to zero. Accordingly, the deflections of the wire at the point of application of the force is

$$w(x = \xi) = \frac{Q(a - \xi)\xi}{Ta} \quad (6)$$

The stiffness of the foundation produced by the systems of wires oriented in the x-direction is now available using the smearing technique:

$$k_2(x, y) = \frac{Q}{w(x = \xi)l_y} = \frac{Ta}{(a - x)xl_y} \quad (7)$$

By analogy,

$$k_1(x, y) = \frac{Tb}{(b - y)yl_x} \quad (8)$$

In the regions of the plate with sparsely located wires, the corresponding stiffness terms can be adjusted replacing the spacing with the Dirac delta function as explained above. The evaluation of damping in a wire as a result of incomplete superelastic hysteresis is discussed in par. 2.2.

Note that for practical manufacturing reasons it may be more convenient to bond the sleeves to the plate at some distance from the boundaries supporting only its central section where vibrations are maximum. In this case the boundaries of the region of the plate supported by prestressed wires are $a_1 < x < a_2$, $b_1 < y < b_2$ as reflected in Fig. 3. This may introduce a limited concentration of inertial contributions of wires and sleeves at the boundary of the supported region, while the counter-pressure produced by wires is absent outside this region. However, the system of wires with sleeves being much lighter than the supported plate, the correction to the inertial term can be disregarded, if the supported region is extended close to the edges of the plate.

The elastic foundation provided by SMA wires does not affect the boundary conditions of the plate. Accordingly, if the edges of the plate are supported by stringers that possess infinite bending and axial stiffness and a negligible torsional stiffness, the corresponding conditions are

$$\begin{aligned} x = 0, \quad x = a : \\ w = 0, \quad \psi_y = 0, \quad M_x = D_{11}(w_{,xx} + \phi_{x,x}) + D_{12}(w_{,yy} + \phi_{y,y}) = 0 \\ y = 0, \quad y = b : \\ w = 0, \quad \psi_x = 0, \quad M_y = D_{12}(w_{,xx} + \phi_{x,x}) + D_{22}(w_{,yy} + \phi_{y,y}) = 0 \end{aligned} \quad (9)$$

It is evident that conditions (9) are identically satisfied by the solution in the form

$$\begin{aligned}
w &= \sum_{m,n} W_{mn}(t) \sin \frac{m\pi x}{a} \sin \frac{n\pi y}{b} \\
\phi_x &= \sum_{m,n} H_{mn}(t) \cos \frac{m\pi x}{a} \sin \frac{n\pi y}{b} \\
\phi_y &= \sum_{m,n} R_{mn}(t) \sin \frac{m\pi x}{a} \cos \frac{n\pi y}{b}
\end{aligned} \tag{10}$$

The substitution of (10) into (1) where the applied pressure is represented

by $q = \sum_{m,n} q_{mn} \sin \frac{m\pi x}{a} \sin \frac{n\pi y}{b} \sin \omega t$, ω being a frequency of the driving pressure and the

application of the Galerkin procedure yields a system of coupled algebraic equations with respect to the amplitudes of the terms in series (10):

$$\begin{aligned}
&\sum_{r,s} \begin{bmatrix} M_{rsmn} & 0 & 0 \\ 0 & I_{rsmn}^{(1)} & 0 \\ 0 & 0 & I_{rsmn}^{(2)} \end{bmatrix} \begin{Bmatrix} \ddot{W}_{rs} \\ \ddot{H}_{rs} \\ \ddot{R}_{rs} \end{Bmatrix} + \sum_{r,s} \begin{bmatrix} C_{rsmn} & 0 & 0 \\ 0 & 0 & 0 \\ 0 & 0 & 0 \end{bmatrix} \begin{Bmatrix} \dot{W}_{rs} \\ \dot{H}_{rs} \\ \dot{R}_{rs} \end{Bmatrix} + \sum_{r,s} \begin{bmatrix} K_{rsmn} & 0 & 0 \\ 0 & 0 & 0 \\ 0 & 0 & 0 \end{bmatrix} \begin{Bmatrix} W_{rs} \\ H_{rs} \\ R_{rs} \end{Bmatrix} + \\
&\begin{bmatrix} F_{mn}^{(11)} & F_{mn}^{(12)} & F_{mn}^{(13)} \\ F_{mn}^{(21)} & F_{mn}^{(22)} & F_{mn}^{(23)} \\ F_{mn}^{(31)} & F_{mn}^{(32)} & F_{mn}^{(33)} \end{bmatrix} \begin{Bmatrix} W_{mn} \\ H_{mn} \\ R_{mn} \end{Bmatrix} = \sum_{rs} \begin{Bmatrix} q_{rsmn}(t) \\ 0 \\ 0 \end{Bmatrix}
\end{aligned} \tag{11}$$

where the coefficients are

$$\begin{aligned}
M_{rsmn} &= \frac{4}{ab} \int_0^a \int_0^b m(x, y) S_{rm}(x) S_{sn}(y) dy dx \\
I_{rsmn}^{(1)} &= \frac{4}{ab} \int_0^a \int_0^b I(x, y) C_{rm}(x) S_{sn}(y) dy dx \\
I_{rsmn}^{(2)} &= \frac{4}{ab} \int_0^a \int_0^b I(x, y) S_{rm}(x) C_{sn}(y) dy dx \\
C_{rsmn} &= \frac{4}{ab} \int_{a_1}^{a_2} \int_{b_1}^{b_2} [c_1(x) + c_2(y)] S_{rm}(x) S_{sn}(y) dy dx \\
K_{rsmn} &= \frac{4}{ab} \int_{a_1}^{a_2} \int_{b_1}^{b_2} [k_1(x, y) + k_2(x, y)] S_{rm}(x) S_{sn}(y) dy dx \\
q_{rsmn}(y) &= \frac{4}{ab} \int_0^a \int_0^b q(x, y, t) S_{rm}(x) S_{sn}(y) dy dx \\
F_{mn}^{(11)} &= A_{55} \left(\frac{m\pi}{a} \right)^2 + A_{44} \left(\frac{n\pi}{b} \right)^2 \\
F_{mn}^{(12)} &= A_{55} \frac{m\pi}{a} \\
F_{mn}^{(13)} &= A_{44} \frac{n\pi}{b} \\
F_{mn}^{(22)} &= D_{11} \left(\frac{m\pi}{a} \right)^2 + D_{66} \left(\frac{n\pi}{b} \right)^2 \\
F_{mn}^{(23)} &= (D_{12} + D_{66}) \frac{m\pi}{a} \frac{n\pi}{b} \\
F_{mn}^{(33)} &= D_{66} \left(\frac{m\pi}{a} \right)^2 + D_{22} \left(\frac{n\pi}{b} \right)^2
\end{aligned} \tag{12}$$

where

$$\begin{aligned}
S_{rm}(x) &= \sin \frac{r\pi x}{a} \sin \frac{m\pi x}{a} \\
C_{rm}(x) &= \cos \frac{r\pi x}{a} \cos \frac{m\pi x}{a}
\end{aligned} \tag{13}$$

Other similar functions are defined by analogy with those in (13).

The integrals that appear in (12), including K_{rsmn} , can be evaluated using a symbolic math program, such as Mathematica. In case where the frequency of the driving pressure is close to the fundamental frequency of the plate so that the analysis can adequately be

conducted using a one-degree of freedom approximation, the integrals K_{rsmn} are evaluated in terms of sine and cosine integral functions. For example, if $r = m = 1$

$$\int_{a_1}^{a_2} k_2(x, y) S_{rm}(x) dx = \frac{Ta}{l_y} \int_{a_1}^{a_2} \frac{\sin^2 \frac{\pi x}{a}}{(a-x)x} dx = \frac{Ta}{l_y} \left\{ \frac{\log a_2 - \log a_1}{2a} - \frac{\log(a_2 - a) - \log(a_1 - a)}{2a} - \frac{1}{2a} \left[Ci\left(\frac{2\pi a_2}{a}\right) - Ci\left(\frac{2\pi a_1}{a}\right) + Ci\left(\frac{2\pi a_2}{a} - 2\pi\right) - Ci\left(\frac{2\pi a_1}{a} - 2\pi\right) \right] \right\} \quad (14)$$

The evaluation of integrals C_{rsmn} does not present difficulties if the equivalent damping is determined as shown in par. 2.2. Other integrals in (12) are also easy to calculate.

A relatively simple approximate solution can be obtained by the Rayleigh-Ritz method. Such solution may lead to approximate expressions for the amplitudes of motion that are convenient for a qualitative analysis of the effect of SMA wires. An example of the Rayleigh-Ritz solution for an isotropic beam supported by a system of wires oriented in the axial direction is shown in the Appendix (to be added to the final version of the paper).

2.2. Equivalent viscous damping for a SMA wire

The equivalent viscous damping of a system of SMA wires reflects the dissipation of energy due to a complete or partial phase transformation of the wire material during vibrations. Representative hysteresis loops of a superelastic SMA material are shown in Figs. 4a,b. Note that a typical strain range corresponding to a complete hysteresis is of an order of several percent, i.e. it requires the motion with exceedingly large amplitudes that are not encountered in structural applications involving composite plates. Therefore, it is anticipated that the wire will experience a partial transformation during vibrations corresponding to the range of strain $2\Delta\varepsilon$ as shown in Fig. 5. This section illustrates the evaluation of an equivalent viscous damping for a representative SMA wire with a prescribed strain range during a cycle of motion.

A wire in the sleeve that is continuously bonded to the plate is shown in Fig. 3. This section illustrates the computation of damping produced by a system of wires parallel to the y-axis, i.e. $c_2(x)$ since the contribution to damping of wires oriented in the x-direction is found through the analogous procedure.

The process described here is iterative, i.e. the deflections of the vibrating plate are assumed known from the previous iteration. In the case of the first iteration it is possible to determine deflections from the solution neglecting the effect of damping. At any

iteration the motion of a wire located at $x = \bar{x}$ is given by $w = \sum_{m,n} W_{mn}(t) \sin \frac{m\pi\bar{x}}{a} \sin \frac{n\pi y}{b}$.

The energy dissipated in the wire during the cycle can be evaluated from the incomplete superelastic hysteresis loop (inner loop) similar to that shown in Fig. 5 using the range of strain specified in the previous iteration. This range is immediately available from

$$2\Delta\varepsilon = 2 \left[\frac{1}{2b} \int_0^b w_{\max}(\bar{x}, y) dy \right]^2 = \frac{1}{2} \sum_n \sum_m \sum_i \left(\frac{n\pi}{b} \right)^2 W'_{mn} W'_{in} \sin \frac{m\pi\bar{x}}{a} \sin \frac{i\pi\bar{x}}{a} \quad (15)$$

where the prime identifies the amplitude values of the corresponding terms obtained in the previous iteration and the factor 2 in front of the square brackets refers to the range, rather than the amplitude value of the strain.

Given static tension in the wire, the pre-strain ε_s is immediately available. Subsequently, the area enclosed within the inner hysteresis loop limited by the strains

$$\varepsilon_{\max} = \varepsilon_s + \Delta\varepsilon, \quad \varepsilon_{\min} = \varepsilon_s - \Delta\varepsilon$$

can be found as

$$\Delta U_d = \int_{V_w} \oint_{\varepsilon} \sigma(\varepsilon) d\varepsilon dV_w \quad (16)$$

where the integration is conducted over the volume of wire V_w . This area represents the amount of energy dissipated by the wire during a cycle of motion. Note that a relatively simple method of calculation of the energy dissipated during a cycle of motion corresponding to an incomplete transformation based on the complex modulus approach was suggested by Gandhi and Wolons⁹.

Let the wire be replaced with a continuous equivalent viscous damper with the damping coefficient C_{wy} . The energy dissipated in such damper during one cycle of motion would be¹⁰

$$\Delta U'_d = \frac{1}{2} \int_0^{2\pi/\omega} \int_0^b C_{wy} \dot{w}^2(\bar{x}, y) dy dt = \frac{b}{4} C_{wy} \int_0^{2\pi/\omega} \sum_{m,n} \sum_{i,n} \dot{W}'_{mn}(t) \dot{W}'_{in}(t) \sin \frac{m\pi\bar{x}}{a} \sin \frac{i\pi\bar{x}}{a} dt \quad (17)$$

The requirement $\Delta U_d = \Delta U'_d$ results in the expression for the damping coefficient of the wire. The hysteresis damping in the wires modeled by smeared or discrete stiffeners can subsequently be determined from (4). Note that the units of C_{wy} found from this

approach are $N^* s / m^2$. This is in agreement with the units in the corresponding equation (1).

2.3. SMA wires in sleeves connected to the plate at discrete points

An alternative approach to design can employ SMA wires in the sleeves, or even without sleeves, connected to the plate at a number of points, rather than along a continuous line. For example, the concentrated force transmitted from the wire to the plate at the attachment points can be found for the cases shown in Figs. 6 and 7.

It is easily shown that the reaction of a wire attached at the mid-point (Fig. 6) and oriented in the x-direction is given by

$$R_{w1} = 2T \left[\sqrt{1 + 4 \left(\frac{w}{a} \right)^2} - 1 \right] \approx 4T \frac{w}{a} \quad (18)$$

The forces transmitted to the plate by a wire attached at three symmetric points (Fig. 7) are

$$R'_{w3} \approx 4T \frac{w_1 - w_2}{a} \quad (19)$$

$$R''_{w3} \approx 2T \left(\frac{w_2}{a'} - \frac{w_1 - w_2}{a''} \right)$$

Therefore, each force can be represented as a linear function of displacements of the points of connection of the sleeve (wire) to the plate. Note that it is assumed that the wires are sufficiently stretched so that their bending between the points of connection to the plate during vibrations can be disregarded.

The elastic reactions of SMA wires can now be represented in terms of functions of deflections of the connection points, so that the reaction at a point (x_i, y_j) supported by wires in both x and y directions is

$$R_w(x_i, y_j, t) = a_{ij} w(x_i, y_j, t) + a_{(i-1)j} w(x_{i-1}, y_j, t) + a_{(i+1)j} w(x_{i+1}, y_j, t) + a_{i(j-1)} w(x_i, y_{j-1}, t) + a_{i(j+1)} w(x_i, y_{j+1}, t) \quad (20)$$

where the subscripts identify the points of wire connection to the plate and the coefficients a_{ij} are easily available.

Collecting the reactions of SMA wires at all connection points the overall reaction of the system of wires can be represented by

$$P_w = \sum_{i,j} k_{ij} w(x_i, y_j, t) \quad (21)$$

where k_{ij} are coefficients dependent on the prestress of wires and the location of the connection points.

The Galerkin procedure applied to the equations of motion yields the following coefficient at the corresponding term in (11):

$$K_{rsmn} = \frac{4}{ab} \sum_{r,s} k_{rs} S_{rm}(x_r) S_{sn}(y_s) \quad (22)$$

The energy dissipated due to damping in a SMA wire experiencing vibrations with the strain range equal to $2\Delta\varepsilon$ is evaluated as explained above (see eqn. 16). The energy dissipated due to an equivalent viscous damping is determined using the velocities of the wire at the connection points. For example, for the wire oriented along $x = \bar{x}$ and connected at N points $x = \bar{x}$, $y = y_k$ ($k = 1, 2, \dots, N$) the energy dissipation due to an equivalent system of viscous damping elements at these points is calculated from

$$\begin{aligned} \Delta U'_d &= \frac{1}{2} \int_0^{2\pi/\omega} \int_0^b C'_{wy} \delta(y - y_k) \dot{w}^2(\bar{x}, y, t) dy dt = \\ & \frac{1}{2} C'_{wy} \sum_k \int_0^{2\pi/\omega} \sum_{m,n} \sum_{i,j} \dot{W}'_{mn}(t) \dot{W}'_{in}(t) \sin \frac{m\pi\bar{x}}{a} \sin \frac{i\pi\bar{x}}{a} \sin \frac{n\pi y_k}{b} \sin \frac{j\pi y_k}{b} dt \end{aligned} \quad (23)$$

Equating the energy dissipation given by (16) to that according to (23) it is possible to evaluate the equivalent viscous damping. The damping pressure applied at all connection points can now be written in the form similar to (21), i.e.

$$p_d = \sum_{i,j} c'_{ij} \dot{w}(x_i, y_j, t) \quad (24)$$

In (24), c'_{ij} is a damping coefficient accounting for equivalent viscous damping produced by all wires connected to the plate at the point $x = x_i$, $y = y_j$.

The term reflecting viscous damping in equations of motion (11) becomes

$$C_{rsmn} = \frac{4}{ab} \sum_{r,s} c'_{rs} S_{rm}(x_r) S_{sn}(y_s) \quad (25)$$

The inertial terms in equations of motion must reflect the fact that wires are connected at a limited number of points (x_i, y_j) . The contribution of the wires in sleeves to rotational inertias can be neglected. If the mass of wires and sleeves at the point (x_i, y_j) is m_{ij} , the mass per unit surface area is

$$\bar{m}(x, y) = \rho_p h + \sum_{i,j} m_{ij} \delta(x - x_i) \delta(y - y_j) = \rho_p h + \frac{m_{ij}}{l_x l_y} \quad (26)$$

Accordingly, the corresponding coefficient in (11) is

$$M_{rsmn} = \rho_p h + \frac{4}{ab} \sum_{ij} m_{ij} S_{rm}(x_i) S_{sn}(y_j) \quad (27)$$

Note that if the plate is thin all previous derivations concerning the stiffness and damping contributions of SMA remain unchanged. The equation of motion becomes

$$D_{11} w_{,xxxx} + 2(D_{12} + 2D_{66}) w_{,xxyy} + D_{22} w_{,yyyy} + m(x, y) \ddot{w} + [c_1(y) + c_2(x)] \dot{w} + [k_1(x, y) + k_2(x, y)] w = q(x, y, t) \quad (28)$$

The deflection represented by the first series (10) satisfies boundary conditions for a simply supported plate. Upon the substitution of the deflection into (28) and the application of the Galerkin procedure the equation of motion is

$$\sum_{rs} [M_{rsmn} \ddot{W}_{rs} + C_{rsmn} \dot{W}_{rs} + K_{rsmn} W_{rs}] + F_{mn} W_{mn} = \sum_{rs} q_{rsmn}(t) \quad (29)$$

where the coefficients M_{rsmn} , C_{rsmn} , K_{rsmn} and $q_{rsmn}(t)$ are not altered compared to the case of a shear deformable plate. The coefficient reflecting the stiffness of the plate is

$$F_{mn} = D_{11} \left(\frac{m\pi}{a} \right)^4 + 2(D_{12} + 2D_{66}) \left(\frac{m\pi}{a} \right)^2 \left(\frac{n\pi}{b} \right)^2 + D_{22} \left(\frac{n\pi}{b} \right)^4 \quad (30)$$

3. Numerical examples

The illustration of the effectiveness of the proposed method was considered on the example of a composite plate supported at the center by two mutually perpendicular SMA wires, each of them parallel to a pair of plate edges. In Figs. 8-10 the cross-ply symmetrically laminated plate was manufactured from AS/3501 graphite epoxy. The example in Fig. 11 is shown for an aluminum Al 2024 plate. The estimated force in the wires was based on the recovery stress of 220MPa recorded by Cross for nitinol¹¹. In case of a 5mm wire diameter, the recovery force in the wire is equal to $T = 4.32kN$. This estimate determined the range of recovery forces considered in the following examples. The plates considered in examples were simply supported and subject to a harmonic pressure distributed over the surface according to the fundamental mode of vibrations.

The following figures illustrate relationships between a nondimensional frequency calculated as a ratio of the driving frequency to the fundamental frequency of the plate without wires and a reduction in the amplitude of motion, i.e. a ratio of the amplitude of the plate with SMA wirers to the amplitude of the same plate without such wires. As follows from Figs. 8 and 9, it is possible to significantly reduce the amplitude of motion of AS/3501 plates using SMA wires. The maximum reduction was achieved at the

fundamental frequency. At lower driving frequencies the effectiveness of the method was reduced but it was still significant even as the driving frequency dropped to 75% of the fundamental frequency value. At higher driving frequencies, the presence of SMA wires that support the center of the plate becomes counterproductive due to the resonance of the plate-wire system whose fundamental frequency is higher than the counterpart of the plate without wires. Predictably, a larger recovery force in SMA wires increases their effect on the amplitude of vibrations. A thinner plate (Fig. 9) is more affected by the presence of wires than a thicker and stiffer counterpart (Fig. 8), even if the recovery force generated in the wires supporting the former plate is smaller.

The effect of the size of the plate on the effectiveness of SMA wires is depicted in Fig. 10. Predictably, larger plates that are relatively less stiff are affected by SMA wires to a larger degree than their otherwise identical but smaller counterparts. Finally, the results for aluminum plates shown in Fig. 11 confirm all conclusions previously discussed in regards to Figs. 8 and 9.

4. Conclusions

The paper presents a methodology of the dynamic analysis of composite and isotropic plates supported by functionally graded SMA wires embedded in sleeves. The solution is obtained for shear deformable plates using the first-order shear deformation theory and for thin plates by the classical plate theory. Two designs of functionally graded SMA reinforcements are considered, including wires in sleeves that are continuously bonded to the surface of the plate and wires attached to the plate at selected points. In the first method, the spacing of wires can be nonuniform to achieve maximum effectiveness for the prescribed amount of SMA. Similarly, in the second case, the points of attachment of SMA wires to the plate can be chosen to maximize their effect.

SMA wires considered in the paper are prestressed through the phase transformation. It is assumed that they operate in the austenitic phase. Accordingly, SMA wires reduce the amplitude of forced vibrations through two mechanisms: (1) resistance to deflections of the structure, i.e. acting similar to an elastic foundation; (2) dissipation of energy as a result of the hysteresis. Although in a realistic range of strain amplitudes SMA wires vibrating with the plate experience an incomplete hysteresis, the dissipation of energy may be significant enough to be included in the analysis.

Numerical examples presented in the paper confirm that strategically placed SMA wires supporting composite and isotropic plates can serve as an effective tool for the reduction of amplitudes of forced vibrations. The wires do not reduce the amplitude of motion for an arbitrary value of the driving frequency. Instead, they effectively “shift” the resonance frequencies of the plate to larger values. Therefore, they should be used selectively, only in applications where the spectrum of driving frequencies is known in advance.

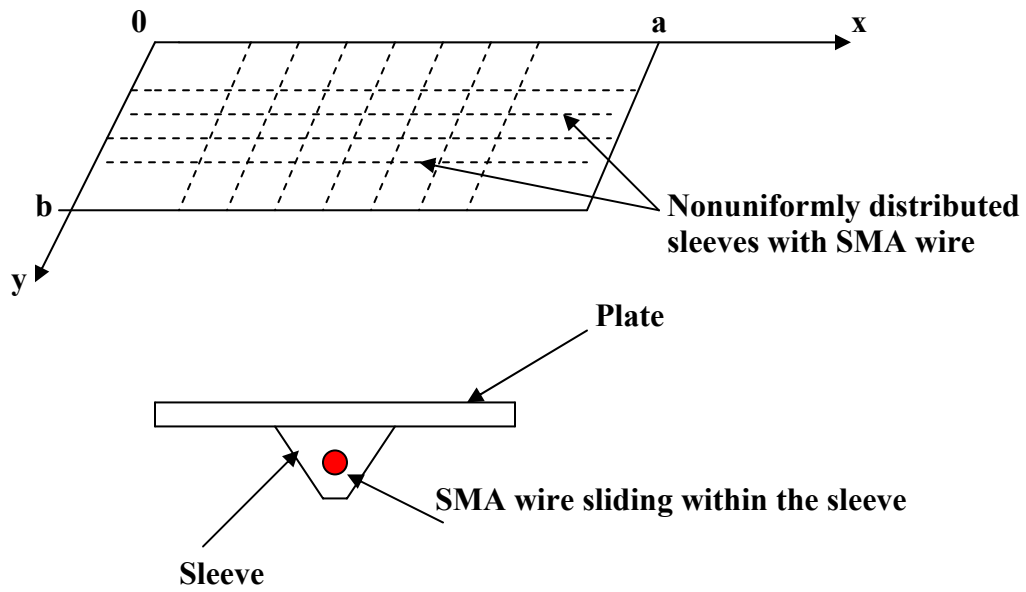


Fig. 1. SMA wires in sleeves bonded with a variable spacing providing a higher support at the central part of the plate. A detail of the cross section with a SMA wire free to slide along the sleeve is also shown.

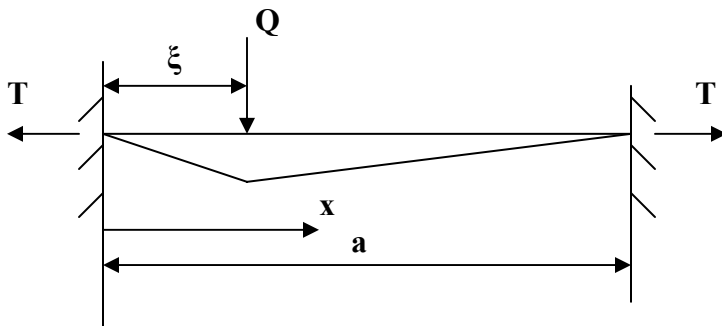
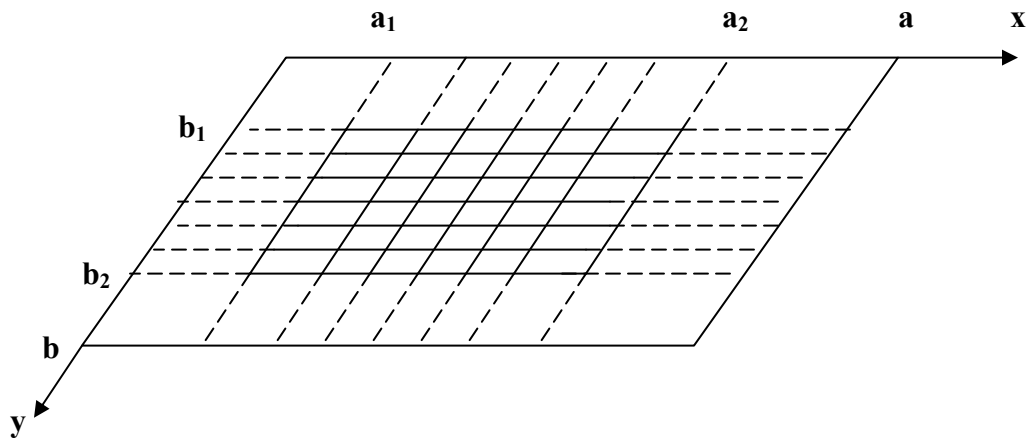


Fig. 2. SMA wire subject to a concentrated force Q at $x=\xi$.



Detail (without supporting boundaries):

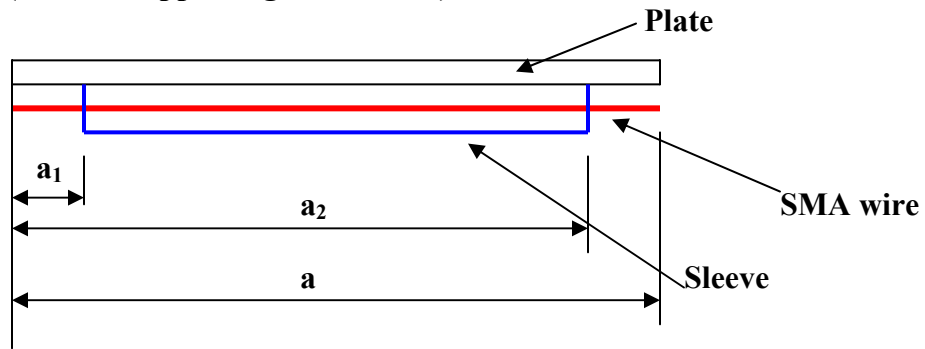


Fig. 3. Plate supported by SMA wires in sleeves within the region $a_1 < x < a_2$, $b_1 < y < b_2$. Solid lines identify wires in the region supported by the sleeves. Broken lines are wires in the unsupported regions.

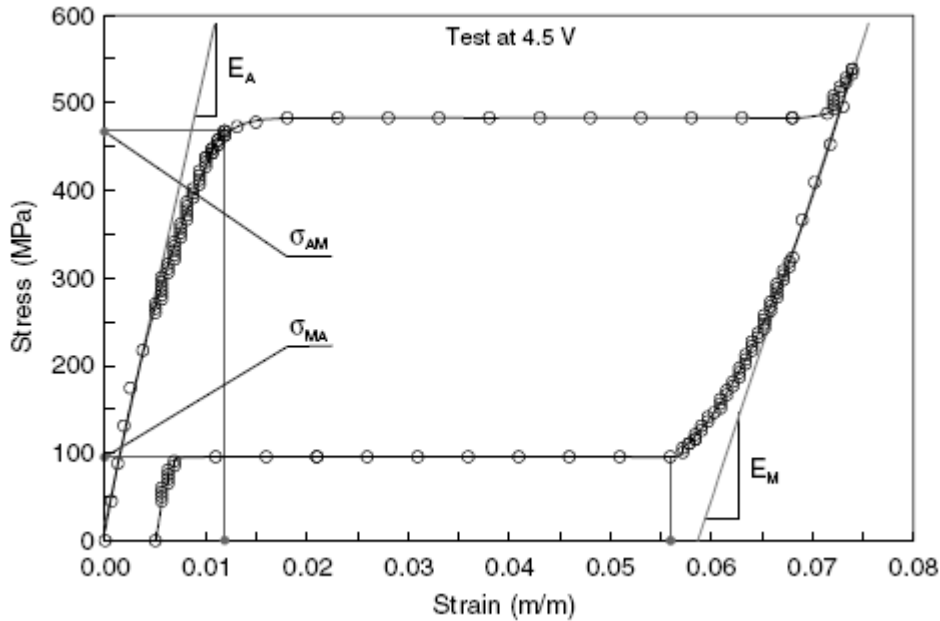


Fig. 4a. A typical hysteresis loop of a Flexinol™ wire (From: Zak AJ, Cartmell MP, Ostachowicz WM and Wiercigroch M, “One-dimensional shape memory alloy models for use with reinforced composite structures,” Smart Materials and Structures, 12, 338-346, 2003).

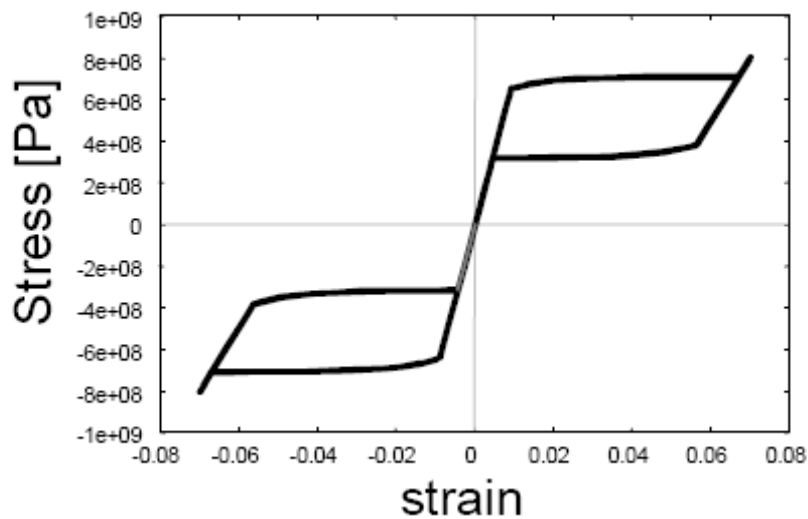


Fig. 4b. A typical hysteresis loop of a NiTi SMA (From: Seelecke S., Heintze O, Masuda, A, “Simulation of earthquake-induced structural vibrations in systems with SMA damping elements,” Proc. SPIE Smart Structures and Materials, 2002, Vol. 4697, San Diego, 2002).

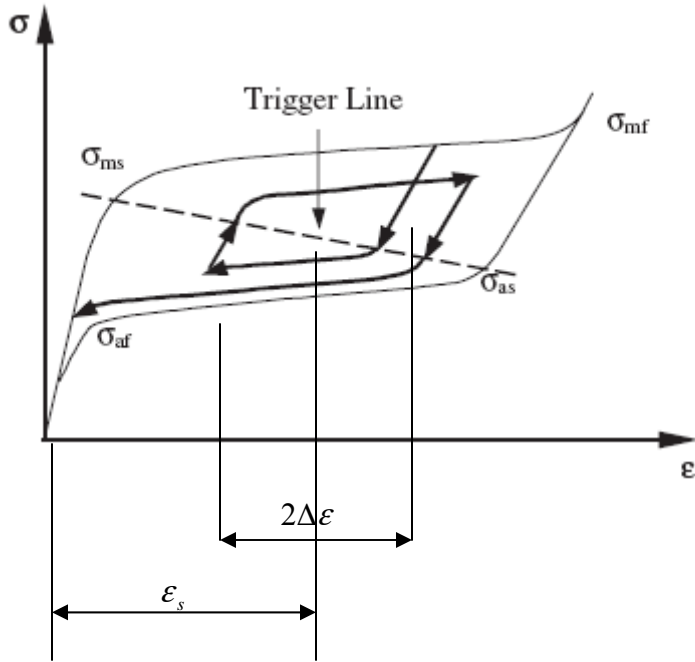


Fig. 5. Dissipation of energy in a prestressed SMA wire vibrating with a prescribed strain range (the corresponding inner hysteresis loop is clearly identified). The energy dissipated per cycle corresponds to the area of the inner loop. The range of strains being prescribed, the area of the loop remains stable during oscillations.

Modified figure from: Saadat S, Salichs, J, Noori M, Hou Z, Davoodi H, Bar-On I, Suzuki Y, Masuda A, "An overview of vibration and seismic applications of NiTi shape memory alloy," *Smart Materials and Structures*, 11, 218-229, 2002.

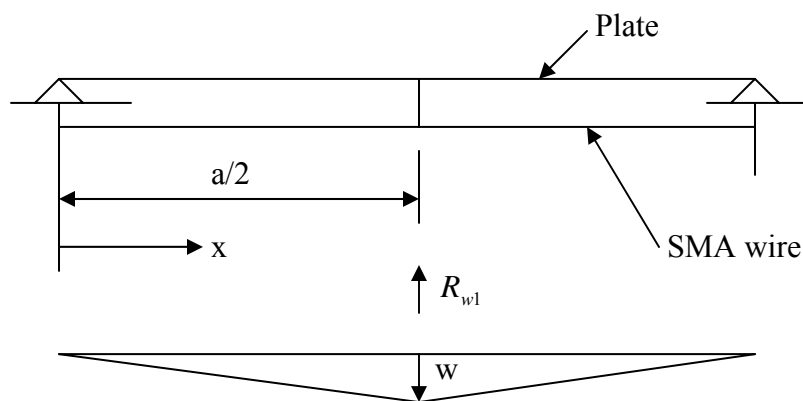


Fig. 6. Prestressed SMA wire connected to the plate at a single central point. The lower figure illustrates a deformed shape of the wire (bending of wire between the supports and

the mid-point is neglected due to prestress and a large difference between its natural frequency and the frequency of the driving load).

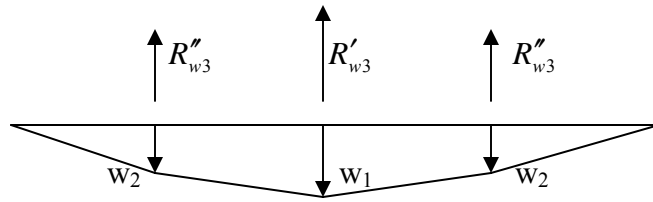


Fig. 7. Deformed shape of a SMA wire connected to the plate at three points.

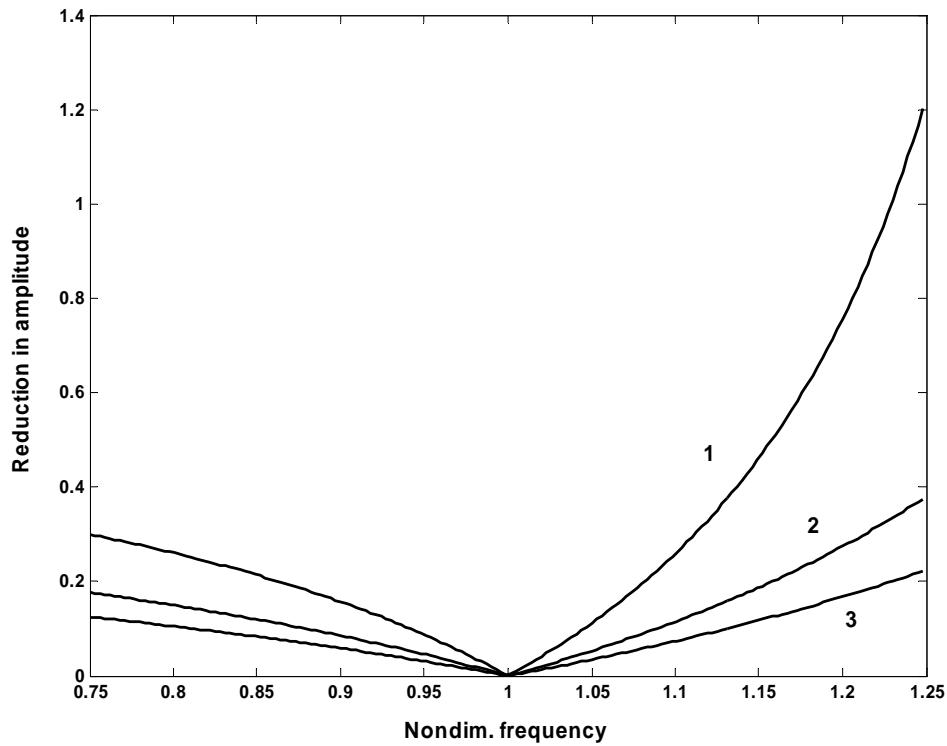


Fig. 8. Effect of SMA wires on the amplitude of vibrations of a square AS/3501 plate ($a = b = 1.0m$, $h = 4.0mm$). Case 1: $T=3.0kN$, case 2: $T=6.0kN$, case 3: $T=9.0kN$.

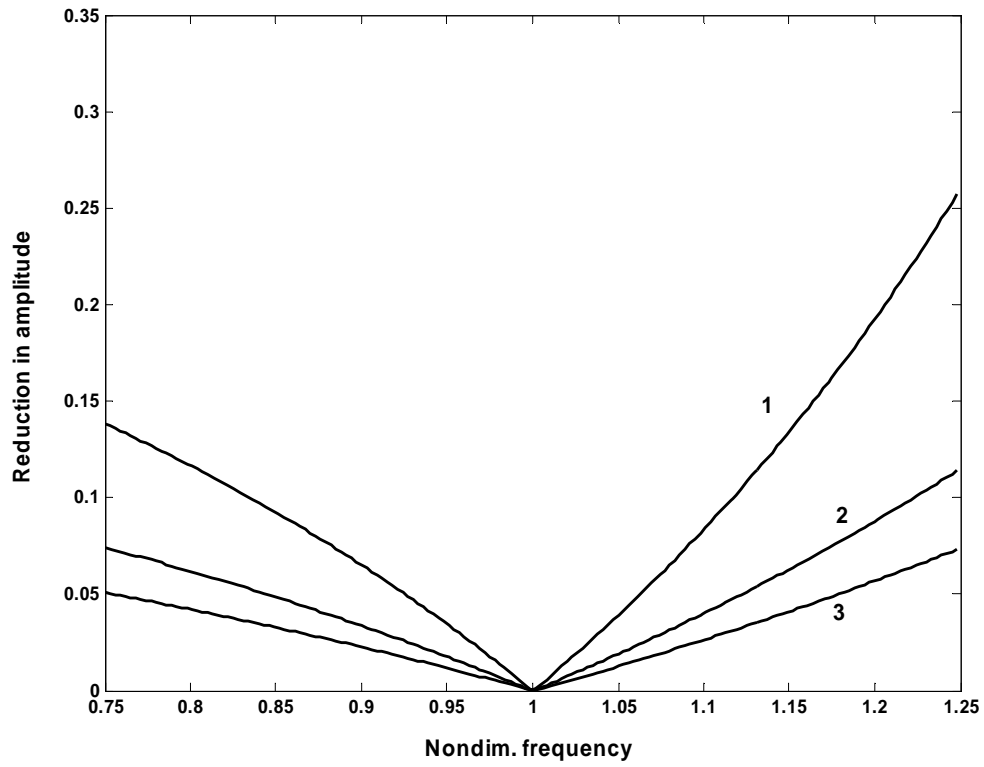


Fig. 9. Effect of SMA wires on the amplitude of vibrations of a square AS/3501 plate ($a = b = 1.0m$, $h = 2.0mm$). Case 1: $T=1.0kN$, case 2: $T=2.0kN$, case 3: $T=3.0kN$.

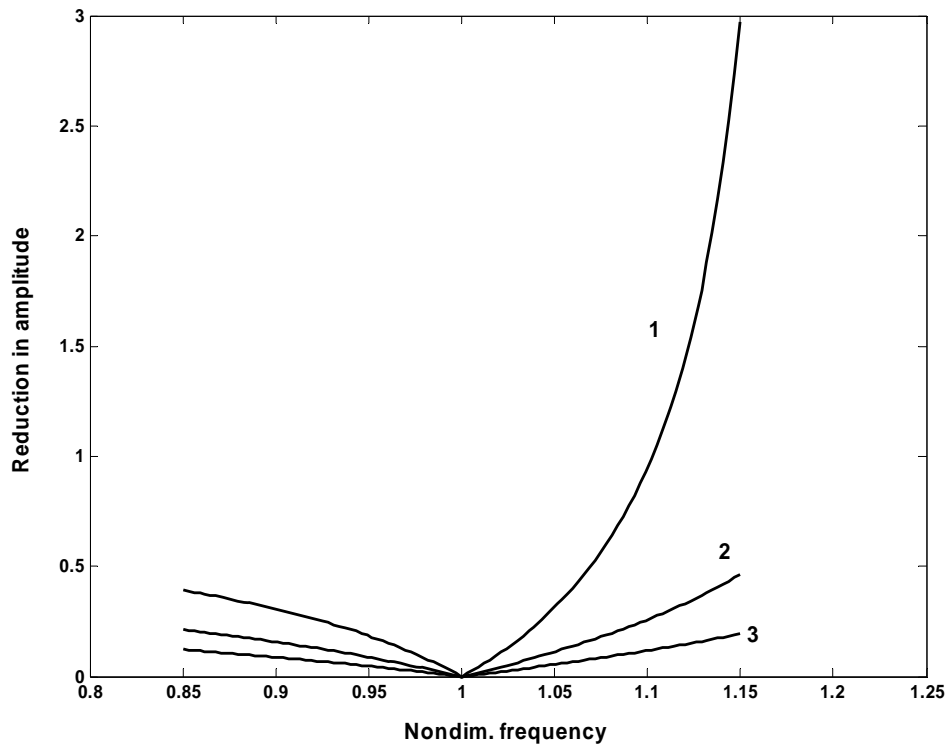


Fig. 10. Effect of the size on the amplitudes of vibrations of a 4mm thick square AS/3501 plate supported with SMA wires with the recovery force equal to 3kN. Case 1: $a=b=0.75\text{m}$, case 2 $a=b=1.0\text{m}$, case 3: $a=b=1.25\text{m}$.

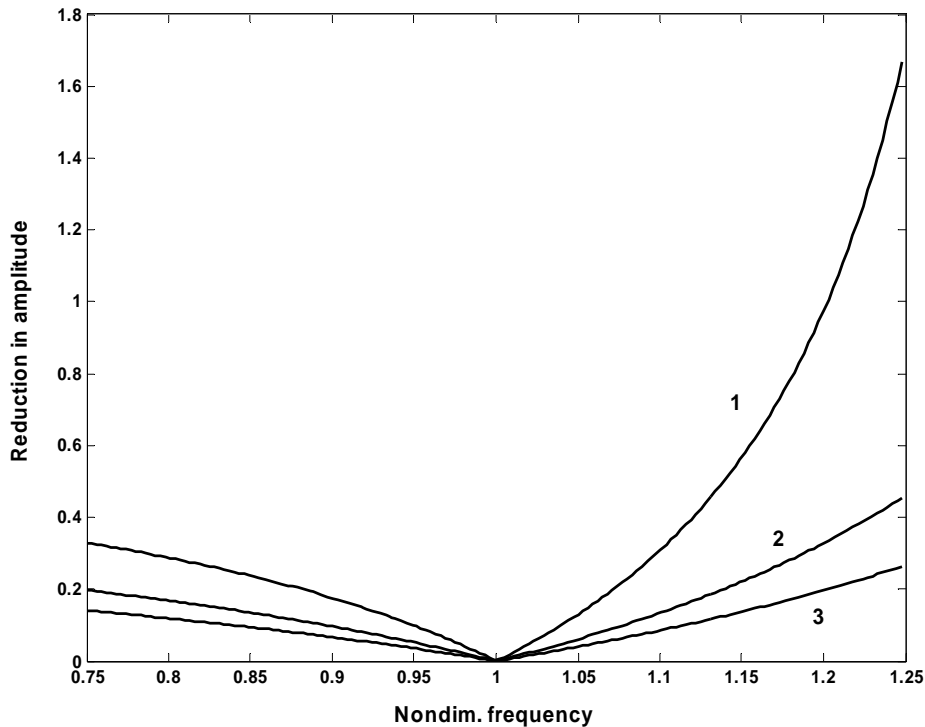


Fig. 11. Effect of SMA wires on the amplitude of vibrations of a square aluminum (Al 2024) plate ($a = b = 1.0m$, $h = 4.0mm$). Case 1: $T=2.0kN$, case 2: $T=4.0kN$, case 3: $T=6.0kN$.

References

- ¹ Birman, V. 1997, Review of mechanics of shape memory alloy structures, Applied Mechanics Reviews, Vol. 50, 629-645.
- ² Baz, A., Poh, J, Ro, J., and Gilheany, J. 1995. Control of the natural frequencies of nitinol-reinforced composite beams, Journal of Sound and Vibrations, Vol. 185, 171-185.
- ³ Ro, J., and Baz, A., 1995. Nitinol-reinforced plates: Part III, Dynamic characteristics, Composites Engineering, Vol. 5, 91-106.
- ⁴ Epps, J and Chandra R. 1997, Shape memory alloy actuation for active tuning of composite beams, Smart Materials and Structures, Vol. 6, 251-264.
- ⁵ Saadat, S., Salichs, J., Noori, M., Hou, Z., Davoodi, H., Bar-On, I., Suzuki, Y., and Masuda, A. 2002, An overview of vibration and seismic applications of NiTi shape memory alloy, Smart Materials and Structures, Vol. 11, 218-229.

⁶ Lagoudas, DC, Khan, MM, Mayes, JJ, and Henderson, BK. 2004, Pseudoelastic SMA spring elements for passive vibration isolation, Part II: simulation and experimental correlations, *Journal of Intelligent Material Systems and Structures*, Vol. 15, 443-470.

⁷ Birman, V. 1997, Theory and comparison of the effect of composite and shape memory alloy stiffeners on stability of composite shells and plates, *International Journal of Mechanical Sciences*, Vol. 39, 1139-1149.

⁸ Reddy, JN. 2004, *Mechanics of Laminated Composite Plates and Shells, Theory and Analysis*, CRC Press, Boca Raton.

⁹ Gandi, F., and Wolons, D. 1999, Characterization of the pseudoelastic damping behavior of shape memory alloy wires using complex modulus, *Smart Materials and Structures*, Vol. 8, 49-56.

¹⁰ Soedel, W. 1993, *Vibrations of Shells and Plates*, Marcel Dekker, New York, p. 319.

¹¹ Cross, WB, Kariotis AH, and Stimler FJ. 1970, Nitinol characterization study. NASA CR-1433.